J. COMBIN. MATH. COMBIN. COMPUT. 127a (2025) 4687--4703

Journal of Combinatorial Mathematics and Combinatorial Computing
www.combinatorialpress.com/jcmcc

Combinatorial Press

Research on cable thermal property detection based on Laplace equation and deep learning fusion algorithm

Ning Zhao[1,✉], Kang Guo[1], Qian Li[1], Siying Wang[1], Ziguang Zhang[1], Lei Fan[1]

[1] State Grid Shijiazhuang Electric Power Supply Company, Shijiazhuang, Hebei, 050000, China

ABSTRACT

This topic is centered around temperature and stress, and describes the theory of electric power thermal characteristics. There are usually two methods for thermal coupling analysis, for direct coupling and sequential coupling. Considering that the stress field of the cable does not have much influence on the temperature field, it is proposed to use the sequential coupling method for the calculation of the thermal characteristics of the cable. The calculated and solved cable temperature and stress distribution values are put into the Lap-ML-ELM algorithm for training. When the contact coefficient k=1, 4, 7, 10, 13 and 15, the cable joints and surfaces produce a monotonically increasing law of temperature, and the stress exhibits the same situation.During the training of the model on the thermal characteristics of the cables, it is found that the accuracy curve of the thermal characteristics detection of the Lap-ML-ELM algorithm is higher than that of both the RNN network and the CNN network, which shows that in the detection of the thermal characteristics of cables, the Laplace Multilayer Extreme Learning Machine fusion algorithm performs more obviously.

Keywords: Laplace equation, ELM, cable, thermal property, detection model

1. Introduction

The Laplace equation is an important partial differential equation that is often used to describe the distribution of potential functions. The Laplace equation has a wide range of applications in physics, engineering and mathematics. In physics, the Laplace equation is usually used to describe the distribution of potential fields [1-4]. Examples include the distribution of electrostatic and static magnetic potentials, and the distribution of velocity and pressure fields in fluid mechanics. In engineering, Laplace's equation is also widely used in the analysis of heat conduction, electric field distribution and other problems [5-7]. And deep learning algorithm is one of the most promising and popular technologies in the field of artificial intelligence in recent years. It simulates the working principle of neural network of human brain and realizes the learning and understanding of complex

✉ Corresponding author.
E-mail address: hbfy_zn@163.com (N. Zhao).
Received 03 March 2024; Revised 20 April 2024; Accepted 10 November 2024; Published Online 15 April 2025.
DOI: 10.61091/jcmcc127a-265

data through multi-level neural network structure [8-11]. The algorithms fused with Laplace equation and deep learning can play an important role in cable detection, and cable thermal characterization is an important part of cable detection.

Cables are important equipment for power supply, communication and data transmission, and their normal operation is crucial for the normal operation of modern society. However, when cables are used for a long time or in harsh environments, various problems may occur, such as broken insulation, broken wires or loose interfaces [12-15]. In order to ensure the safety and reliability of the cable, timely cable testing is very necessary. Cable testing can be divided into online testing and offline testing of two kinds [16-17]. Online detection refers to the normal operation of the cable in the process of its detection. This detection method does not need to interrupt the use of cable, real-time monitoring of cable performance parameters, such as resistance, voltage, etc.. Online testing can be carried out through specialized cable testing equipment, but also through remote monitoring system [18-21]. Offline testing refers to the cable from the power supply system is removed, for detailed testing and analysis. This type of testing allows for a more comprehensive examination of the physical and electrical properties of the cable, such as insulation resistance, voltage withstand, leakage current, and so on. Off-line testing can be performed by laboratory equipment or non-destructive testing [22-25].

An algorithm for cable damage detection based on the Hilbert transform of induced guided ultrasound recorded signals was proposed in the literature [26]. Its applicability to multiple types of cables and the possibility of damage identification by evaluating wave amplitude values were also examined. Literature [27] describes the understanding and progress of inspection, monitoring and evaluation of bridge cables, including damage types and detection techniques. Research directions and challenges are envisioned. Provides reference for future research and innovation in bridge cable inspection, maintenance and management. Literature [28] analyzed the application of ultrasonic guided waves in cable defect detection. It was emphasized that in the pulse-echo configuration, the defect detection coverage was expanded, proving the effectiveness of ultrasonic guided waves. Literature [29] outlines the forms of cable termination faults found by field operators and researchers, and the methods typically used to detect cable termination faults. It helps to provide a reference for novices and provides a comprehensive summary of trends in cable terminal defect detection methods. Literature [30] describes wireless distributed sensors for monitoring external disturbances in cables. By carrying out vibration tests, the time domain and time-frequency characteristics of cable vibration signals are obtained, which lays the foundation for the establishment of an intelligent early warning system for cable breakage resistance. Literature [31] proposed a fusion prediction model for life prediction of submarine cables by using an analytical model supported by accelerated aging data. And the results of low-frequency sonar analysis of submarine cables are presented, aiming to monitor the cables. And by integrating and validating these sonar data, the remaining service life of the cable can be predicted.

The above study describes various techniques and methods used in cable inspection such as ultrasonic waves and highlights the effectiveness of these methods and their impacts, whereas with the gradual maturation of robotics research and development techniques, robots are gradually being used in various fields, and there is no exception in cable inspection. Literature [32] discusses the application of robots in cable inspection. And based on the discussion of traditional inspection methods and robots, the expected budget of cable inspection robots was examined. Literature [33] points out the limitations of current cable condition inspections and proposes the use of robots in in cable inspection. The effectiveness of the robot in cable inspection is emphasized by improving its climbing ability. Literature [34] discusses the intelligent cable trench inspection robot in cable inspection. A path planning method combining the improved a* algorithm with DWA and an underground cable trench condition assessment method were also proposed. It reveals that the robot can effectively acquire detection information as well as the effectiveness of this assessment method. Literature [35] developed a small urban cable duct inspection robot prototype. The robot's support module was able to effectively prevent tilting in the conduit, achieving the desired design goals and improving the quality control of cable laying. Although emerging technologies such as robotics have been applied in cable inspection, but as far as the current research is concerned, based on the Laplace equation and deep learning fusion algorithm in cable inspection and is reflected.

In this paper, combining the basis of Laplace equation and deep learning theory, the Laplace multilayer extreme learning machine is proposed to explore the cable thermal characteristic detection. Combined with the actual working principle of the cable, the theory of thermal characteristics of the cable can be divided into the theory of temperature characteristics and the theory of stress characteristics. Since the use of direct coupling will lead to the situation that the temperature field and the stress field interfere with each other, accordingly the sequential coupling method is used to calculate the temperature and stress distribution value of the cable. The values are put into the Laplace multilayer extreme learning machine fusion algorithm as inputs for training, and the model training performance is evaluated and analyzed, aiming to test the model's ability to detect the thermal characteristics of cables.

2. Cable Thermal Characterization Program

2.1. Laplace's Equation and Deep Learning Fusion Algorithm

2.1.1. Fundamentals of the Laplace equation. It is well known that the Laplace equation is one of the simplest elliptic partial differential equations. To wit:

$$\frac{\partial^2 u}{\partial x^2}+\frac{\partial^2 u}{\partial y}=0 \tag{1}$$

From the physical point of view, the equation describes a steady-state phenomenon, such as the distribution of temperature inside a flat metal plate at a given boundary temperature [36-38]. Boundary conditions for elliptic partial differential equations can be formulated in the following three ways: (1) Fixed boundary conditions, i.e., the value of u is given on a given boundary, $U_1(x,y)$. (2) Normal derivative values of u are given on a given boundary, $\partial u/\partial n = U_2(x,y)$. (3) Mixed boundary conditions are given on a given boundary, $\partial u/\partial n_+ u = U_3(x,y)$. Of these, the first one is the most commonly provided, and the algorithm is validated in this subsection with the first formulation. The following computational domain boundaries as well as boundary conditions are given:

$$\begin{cases} 0\le x\le 2, 0\le y\le 2 \\ u(0,y)=0, u(2,y)=y(2-y) \\ u(x,0)=0, u(x,2)=\begin{cases} 2-x & x>1 \\ x & x<1 \end{cases} \end{cases} \tag{2}$$

The one-dimensional convection equation is a typical first-order hyperbolic partial differential equation with the following form:

$$\frac{\partial u}{\partial t}+\alpha\frac{\partial u}{\partial x}=0 \tag{3}$$

where a is a nonzero constant. We know that it is hyperbolic and given the initial conditions, its solution is unique. Without loss of generality, here let $a=-1$ and given the following initial conditions:

$$u_0(x)=\begin{cases}10x+1,-0.1\le x\le 0\\-10x+1,0\le x\le 0.1\\0,-0.1>x\text{ or }x>0.1\end{cases}\tag{4}$$

The initial signal is triangular with width 0.2 and discontinuous first order derivative at $x=0$. In order to check the accuracy of the algorithm in this paper, the algorithm in this paper and the finite difference windward format algorithm are used to solve the initial value problem of the above hyperbolic partial differential equation respectively. Ideally, the solution should result in triangular signal shapes distributed at different spatial locations at different moments.

2.1.2. Laplace Multilayer Extreme Learning Machine (Lap-ML-ELM).In this paper, Laplace's equation is fused with multilayer polar learning machine in the context of deep learning algorithms, which can be used for subsequent cable thermal exploration. The regularization framework based on multilayer polar learning machine is currently a hot topic in deep learning research, which utilizes the streamform assumption, which takes the labeled and unlabeled samples as the vertices of the data graph, and the edges of the vertices as the weights, and if two samples x_i and x_j are close to each other, their labels y_i and y_j should be close to each other as well, and in order to achieve this assumption, the streamform regularization framework minimizes the cost function in the first instance:

$$L_m=\tilde{Y}^T L\tilde{Y}\tag{5}$$

where $\tilde{Y}=\left[\vec{y}_i,\vec{y}_j\right]$, D are diagonal matrices and L is the Laplace equation matrix.

We introduce the streamform regularization framework into the multilayer extreme learning machine model and propose the Laplacian multilayer extreme learning machine Lap-ML-ELM.The structure of the Lap- ML-ELM model is the same as that of the ML-ELM, but the Lap-ML-ELM trains labeled samples together with unlabeled samples. The biggest difference between the Lap-ML-ELM and the ML-ELM is that the final output weights β are derived differently: the ML-ELM is derived directly by minimizing a generalized regularized cost function of least squares estimation, and the Lap-ML-ELM is derived using a streaming regularization framework. In semi-supervised learning, we have a small number of labeled samples $\{X_l,Y_l\}=\{x_i,y_i\}_{i=1}^{l}$, and a large number of unlabeled samples $X_u=\{x_i\}_{i=1}^{u}$, and Lap-ML-ELM takes the labeled and unlabeled samples and trains them layer-by-layer using ELM pairs. Assuming that Lap-ML-ELM has k hidden layers, the output of the k th hidden layer can be found by taking the 6th hidden layer output H_k by Eq. We find the output weights β by minimizing the following cost function. i.e:

$$\min L_{Lap-ML-ELM}=\frac{1}{2}\|\beta\|^2+\frac{C}{2}W\|Y-H_k\beta\|^2+\frac{\lambda}{2}Tr\left(\beta^T H_k^T LH_k\beta\right)\tag{6}$$

where C is the external regularization parameter, λ is the intrinsic regularization parameter, $Y\in R^{(l+u)\times m}$ consists of the labels Y_l of the labeled samples and the labels $Y_u=0$ of the unlabeled samples, and W is the diagonal matrix of $(l+u)\times(l+u)$, with the diagonal elements of the first l being $W_{ii}=1/N_i$ and the rest 0.

If the derivation of $L_{Lap-ML-ELM}$ is equal to 0, then we get:

$$\beta-CH^TW\left(Y-H_k\beta\right)+\lambda H_k^T LH_k\beta=0\tag{7}$$

The output weight β can be obtained by the following equation:

$$\beta=\begin{cases}\left(1+CH_k^TWH_k+\lambda H_K^T LH_k\right)^{-1}H_k^T CWY,1+u\ge n_k\\H_k^T\left(1+CWH_kH_k^T+\lambda LH_kH_k^T\right)^{-1}CWY,l+u<n_k\end{cases}\tag{8}$$

where n_k is the number of nodes in the k nd hidden layer in Lap-ML-ELM.

2.2. Theory of thermal properties of cables

2.2.1. Theoretical analysis of temperature characteristics. The high temperature from the arc is the main heat source, and heat propagation occurs throughout the cable work, with heat spreading both between the fused cladding layers by heat conduction and spontaneously with the forming environment by convection and radiation at the surface and ends. At the same time, the heat dissipation changes as the experimental process continues. Thus the temperature of the molding process is in a constant state of flux. Temperature changes result in thermal stresses, while deformation of the formed part occurs, causing the temperature to change continuously, and a coupled analysis of the thermal properties must be carried out in order to improve the accuracy of the simulation solution. The following is an analysis of various heat transfer methods:

1) Heat conduction. The essence of heat conduction is completely in contact with each other between the two objects or based on the same object in different parts of the temperature distribution is not uniform and triggered by the conversion of thermal energy, this way requires a medium, and the propagation of heat follow Fourier's law. For the thermal characteristics of the cable, heat conduction occurs mainly between the fusion cladding and the melting process of the wire and the experimental substrate.

2) Convective heat transfer. The essence of convective heat transfer between the fluid and its mutual contact with the solid surface, and due to the temperature difference induced by different locations of heat transfer, the academic use of Newton's cooling formula to calculate the size of the heat and the direction of propagation in this way. Cable part of the heat will be transferred to the molded parts and substrates in this way.

3) Thermal radiation. All objects every moment to the outside world in the radiation of heat, the essence of its occurrence is the object to the outside world to emit electromagnetic waves are absorbed by the outside world into the savings of internal energy. Thermal radiation does not require any medium, the cable part of the heat will be dissipated by thermal radiation.

For the temperature of the cable and the characteristics of the spatial distribution of heat flow with time, the Laplace equation is used to characterize the universal law of the three-dimensional heat propagation process of the cable, based on the principle of conservation of energy and without taking into account the internal dynamic response of the molten metal layer:

$$\rho C_p \frac{\partial T}{\partial t} = \frac{\partial}{\partial x}(\lambda \frac{\partial T}{\partial x}) + \frac{\partial}{\partial y}(\lambda \frac{\partial T}{\partial y}) + \frac{\partial}{\partial z}(\lambda \frac{\partial T}{\partial z}) + \bar{Q} \tag{9}$$

In the formula:

ρ - density of the material, $\mathrm{kg \cdot m^{-3}}$.

C_p - Specific heat capacity of the material, $\mathrm{J/kg \cdot {}^\circ C}$.

λ - thermal conductivity of the material, $\mathrm{W/m \cdot {}^\circ C}$.

T - temperature, $\mathrm{{}^\circ C}$.

t - Heat propagation time of the additive molding process, s.

x, y, z - a position inside the heat source, m.

$\bar{Q}$ - Energy intensity at a point inside the heat source, $\mathrm{W/m^3}$.

Boundary conditions are the key to a definite solution of the partial differential equation, and the solution of the partial differential equation (10) depends on the following thermal field boundary conditions:

1) The temperature on the boundary of the molded part is known:

$$T_s = T_s(x, y, z, t) \tag{10}$$

2) The heat flow density at each point of the boundary of the molded part is known:

$$\lambda \frac{\partial T}{\partial n} = q(x, y, z, t) \tag{11}$$

3) The heat exchange between the boundary of the molded part and its surrounding medium is known:

$$\lambda \frac{\partial T}{\partial n} = \alpha (T_\alpha - T_0) \tag{12}$$

Eq:

$\frac{\partial T}{\partial n}$ - Temperature gradient of temperature on the boundary surface.

α - coefficient of heat transfer on the surface of the molded part, $\mathrm{W/m^2 \cdot {}^\circ C}$.

T_α - temperature on the boundary surface of the molded part, $^\circ\mathrm{C}$.

T_0 - temperature of the surrounding medium, $^\circ\mathrm{C}$.

Cable thermal properties and welding technology has a similarity, can be calculated with the help of the relevant approach to solving the latent heat of phase change, usually solve the latent heat of the material contains enthalpy method, the apparent heat capacity method, the equivalent heat fusion method, as well as the method of temperature recovery, etc., and this paper is mainly used in the equivalent heat fusion method. Equivalent hot melt method: The principle is similar to the sensible heat capacity method, which is formed by the superposition of the specific heat capacity of the wire itself and the specific heat generated by the latent heat of phase change. Among them, the former can be obtained by looking up the table, the latter can be calculated by the formula (13) and (14). Namely:

$$C_1 = \frac{L}{T_1 - T_s} \tag{13}$$

$$C_{pe} = C_p + C_1 \tag{14}$$

In the formula:

L - Latent heat of the molded part, $\mathrm{J/kg}$.

C_{pe} - equivalent specific heat capacity, $\mathrm{J/kg \times {}^\circ C}$.

2.2.2. Theoretical analysis of stress characteristics.The difference between the thermal characterization of cables and common welding techniques is obvious, mainly in the fact that the process of thermal characterization of cables is regional and temporal. Under the influence of the movement of the heat source, the layers constrain each other, forming a complex temperature change in the body of the molded part. Various forms of stresses are coupled during the cooling time, which ultimately limits the surface morphology, molding accuracy and mechanical properties of the component. The total (equivalent) stresses generated in cables are the result of the superposition of various stresses, mainly by means of the finite element method and the intrinsic strain method, for the study of cable stress characteristics. Firstly, the total strain consists of elastic strain, thermal strain, plastic strain and strain due to phase transformation, etc. Secondly, according to the generalized Hooke's law, the equivalent stresses on the internal components are superimposed by the component stresses corresponding to these strains.

1) Yield criterion:

$$\bar{\sigma} = \frac{\sqrt{2}}{2} \sqrt{(\sigma_1 - \sigma_2)^2 + (\sigma_2 - \sigma_3)^2 + (\sigma_1 - \sigma_3)^2} \tag{15}$$

$$\bar{\varepsilon} = \frac{\sqrt{2}}{2(1+\mu)} \sqrt{(\varepsilon_1 - \varepsilon_2)^2 + (\varepsilon_2 - \varepsilon_3)^2 + (\varepsilon_1 - \varepsilon_3)^2} \tag{16}$$

In Eq:

$\sigma_1, \sigma_2, \sigma_3$ - Principal stress of the formed part along the forming direction.

$\varepsilon_1, \varepsilon_2, \varepsilon_3$ - the principal strain of the molded part in the direction corresponding to the principal stress.

2) Flow criterion:

$$\{d\varepsilon\}_p = \xi \frac{\partial \bar{\sigma}}{\partial \{\sigma\}} \tag{17}$$

In Eq:

ε - the principal strain of the metallic material.

ξ - Quantity factor.

2.3. Coupling of thermal properties

This subsection calculates the thermal coupling performance of the cable and analyzes the mechanical properties of the structure with different design parameters under thermal and compressive loading conditions to provide data support for the subsequent testing of the thermal properties of the cable.

2.3.1. Sequential coupling.There are two general approaches to thermal coupling analysis: direct coupling and sequential coupling. Direct coupling requires the use of a coupled unit type that contains all physical degrees of freedom and uses only one solver. This method solves for both the temperature and stress fields of the cable, and is used in cases where the temperature and stress fields have a very large influence on each other. Sequential coupling first calculates the temperature field of the structure under thermal loading, and then the temperature field obtained from the solution is applied as a boundary condition to the solution process of the stress field, which is simpler and more convergent than direct coupling. In this paper, considering that the stress field of the cable has little influence on the temperature field, in order to facilitate the calculation, the sequential coupling method is used to calculate the thermal characteristics of the cable.

2.3.2. Coupling process.Sequential thermal coupling can be divided into the following steps:

1) Establish a heat transfer unit model of the cable, apply thermal loads and thermal boundary conditions, perform transient or steady-state thermal analysis of the cable, and solve to obtain the temperature field of the structure under thermal loads.

2) Establish the stress unit model of the structure, define the mechanical properties of the material, apply mechanical loads and boundary conditions to the decoupled strands, and apply the temperature field obtained from (1) as the boundary conditions, and finally carry out the stress calculation on the structure.

In order to consider its generality, thermal loads are applied to the upper surface of the cable, the parameters in the heat transfer model are determined, and the temperature field results for the heat transfer of the cable are calculated.

For the stress analysis, the static, generic analysis steps Step1 and Step2 are created with the boundary conditions: the initial temperature field of the cable is 293 K. Then the temperature field of the results of the heat transfer calculation of the cable is loaded as a temperature load into the Step1 analysis step and a fixed load is applied to the lower panel, and finally the upper surface is set up to apply the compressive load P in the Step2 analysis step.

2.4. Cable Thermal Characterization Model

In order to improve the accuracy of the cable sequential thermal coupling results, the cable temperature and stress distribution values are solved by sequential coupling, which are used as the input features of the Lap-ML-ELM model, and the Adam optimization algorithm is used to iteratively train the features to ensure the stability and accuracy of the model in different scenarios. The trained model is deployed to the actual scene to analyze and process the real-time collected cable data. Based on the model output, it determines whether there is a fault in the cable as well as the problem and severity of the fault, providing decision support for repair and maintenance.

3. Cable thermal characterization and testing

3.1. Thermal characterization of cables

3.1.1. Calculation and analysis of thermal-force characteristics.Figure 1 shows the three-dimensional temperature distribution of the cable joint, where (a) to (c) are the temperature field cloud, cross-section at z=2700 mm, and cross-section at z=4800 mm, respectively. The temperature distribution results from the figure can be seen:

1) The temperature at the cable joint conductor connection is the highest, reaching 58.268°C.

2) The temperature of the cable core conductor in the cross-section at z=3000 mm and z=5500 mm is 58.267°C and 58.268°C, respectively, and the temperature of the cable core conductor in the center of the joint is 9.31% higher than that in the body. The corresponding surface temperatures were 41.723°C and 58.427°C, and the surface temperature at the center of the joint was 12.721% lower than that at the body. The reason for this phenomenon is due to the large outer diameter of the cable connector, resulting in a larger heat dissipation area and a correspondingly higher convective heat dissipation capacity.

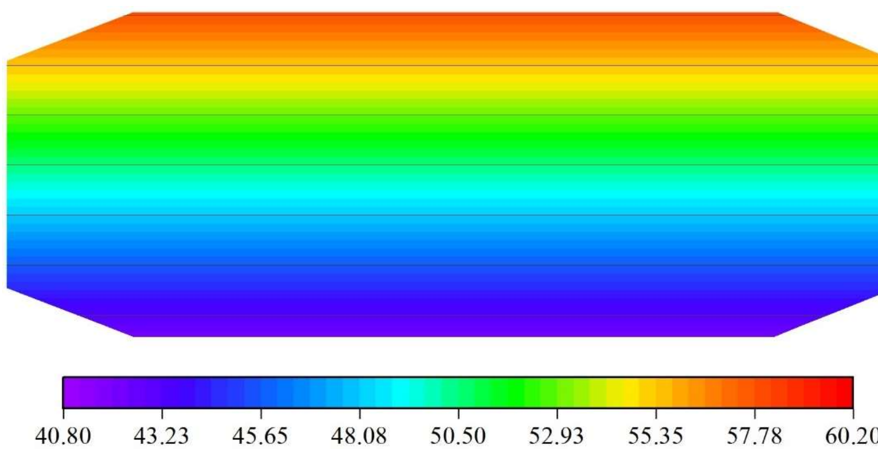

(a)Temperature field cloud picture

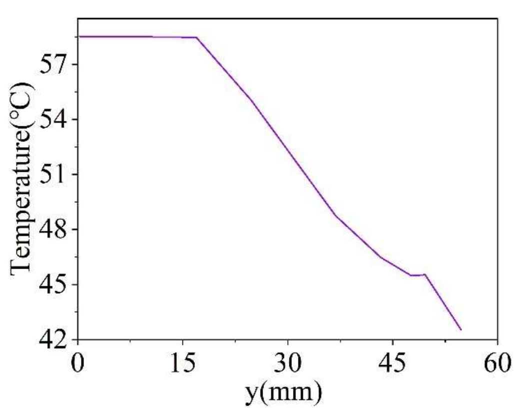

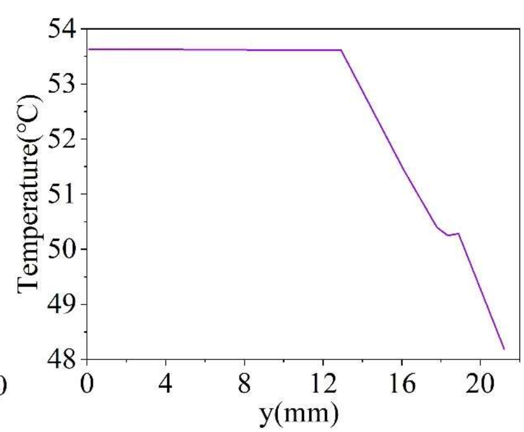

(b)z=2700 mm cross section (c)z=4800 mm cross section

Fig. 1. Three-dimensional temperature distribution of cable joints

Fig. 2 shows the axial distribution curve of cable core conductor and surface stresses in cable joints, where (a)~(b) are the cable core conductor and surface, respectively. z=3000 mm at the center of the joint cable core conductor stress is smaller than that at the body, which is due to the fact that at the center of the joint, the highly elastic prefabricated rubber material on the outer side of the cable conductor is subjected to thermal expansion and produces compressive stresses on the cable core conductor, whereas in the body of the cable, the compressive stress is less. The compressive stress is smaller at the cable body. The surface of the cable joint is a free boundary condition, not subject to other external forces, and its stress is closely related to its own temperature. As the surface temperature of the cable joint is smaller than the body surface temperature, so that the center surface stress of the cable joint is also smaller than the body at the surface stress.

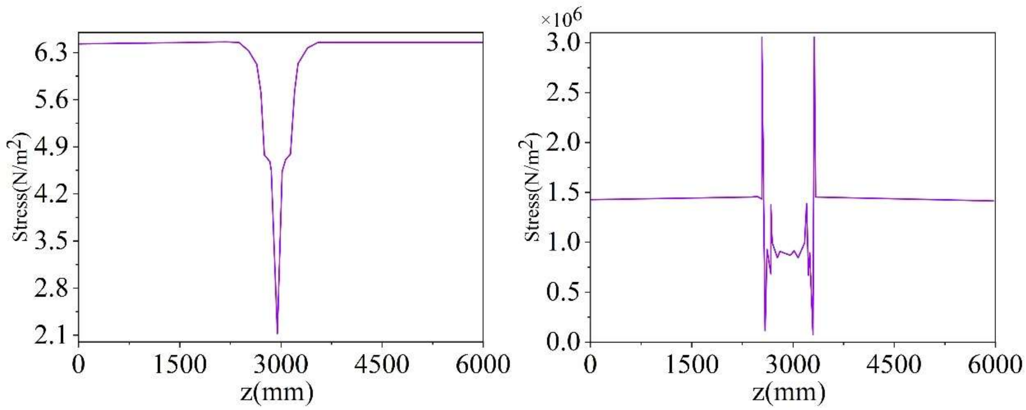

(a) Cable core conductor (b)Surfaces

Fig. 2. Cable stress axial distribution curve

3.1.2. Temperature Characterization

1) The effect of contact coefficient k on temperature characteristics. When the contact coefficient k = 1, 4, 7, 10, 13 and 15, the temperature distribution curve of the core of the cable joint is calculated as shown in Figure 3. As the contact coefficient k increases, z = 3000 mm at the center of the joint cable core conductor temperature increases, and the magnitude of the temperature increase is also a small increase. For example, when the value of contact coefficient k increases from 1 to 4, the temperature increases from 48.9°C to 53.99°C, which is an increase of 5.09°C, while when the value of contact coefficient k increases from 10 to 13, the temperature increases from 69.09°C to 74.37°C, which is an increase of 5.56°C. The conductor temperature of the cable body core at z=5500 mm remains almost unchanged as the contact coefficient k increases. This is because the heat conduction along the axis of the cable core within the range of z<500 mm and z>5500 mm has become very weak, making the temperature of the cable body core 2.5 m from the center of the connector negligible by the change in the contact coefficient k of the connector. As the value of the contact coefficient k increases, it makes the volumetric heat generation rate of the equivalent conductor at the joint connection increase, but the larger outer diameter size of the joint makes the convective and radiative heat dissipation between its surface and the air stronger.

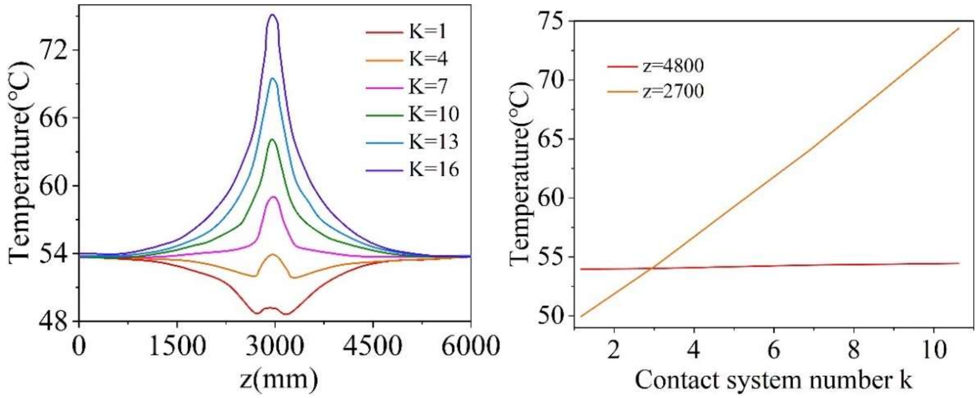

(a) Distribution along the axis (b) z=4800 and 2700mm

Fig. 3. Temperature distribution curves of cable core with different k

The cable core conductor is a good conductor of heat, and there is only a temperature gradient along the axial direction, but the value of this temperature gradient is much smaller than the value of the temperature gradient on the surface of the cable. Therefore, the cable joint surface temperature gradient law is analyzed. Figure 4 gives the distribution curve of the temperature gradient on the cable surface under different values of contact coefficient k. Since the cable surface radial temperature gradient is a linear function of the surface temperature. So that the cable surface temperature gradient distribution curve in Figure 4 and the cable surface temperature distribution curve in Figure 3 have the same shape and change rule.

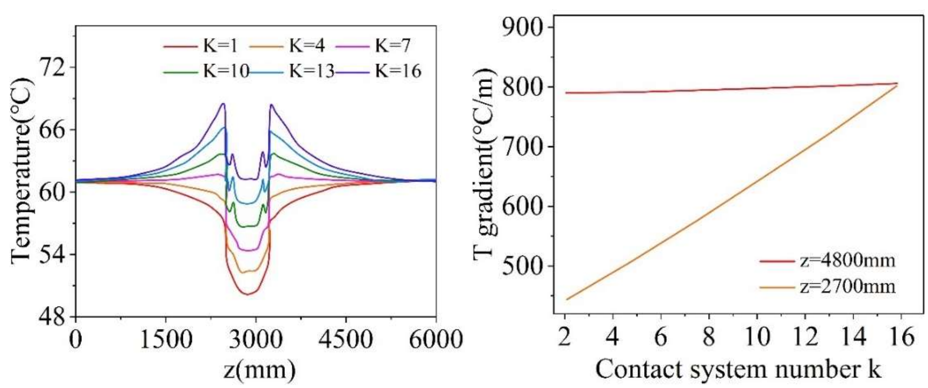

(a) Distribution along the axis (b) z=4800 and 2700mm

Fig. 4. Temperature gradient distribution curves of cable surface with different k

2) The influence of ambient temperature on temperature characteristics. Keep the load cable I = 638A and contact coefficient k = 7 unchanged, calculate the ambient temperature Tamb were 10, 15, 20, 25, 30 and 35 ℃ cable core and surface temperature distribution curve shown in Figure 5 and Figure 6, respectively. Cable core and surface temperatures are with the ambient temperature Tamb rise and rise, the ratio between its temperature rise and the environmental temperature rise is approximately constant, i.e., the ambient temperature Tamb every 1 ℃, the cable core conductor and the surface of the temperature of each part of the cable core is also correspondingly increased by 1.17 ℃. z = 4800mm and z = 2700mm at the cable cable core conductor temperature difference and the surface temperature difference of the cable by the ambient temperature Tamb change has less influence, respectively. Tamb change has less influence, respectively, about constant 5.244 ℃ and 6.443 ℃.

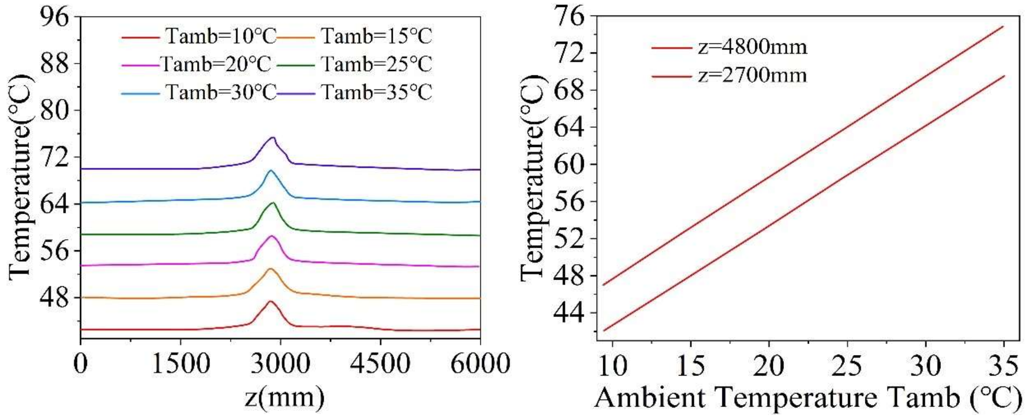

(a) Distribution along the axis (b) z=4800 and 2700mm

Fig. 5. Temperature distribution curve of cable core

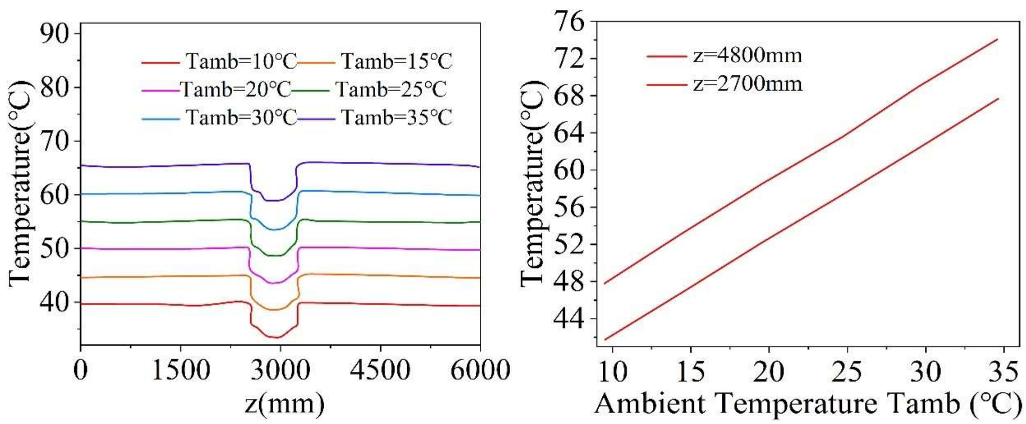

(a) Distribution along the axis (b) z=4800 and 2700mm

Fig. 6. Cable surface temperature distribution curve

3.1.3. Analysis of Stress Characterization Laws

1) Influence of contact coefficient k on stress characteristics. The contact coefficient k at the cable joints directly affects the distribution of its temperature field, but also an important factor affecting the distribution of the thermal stress field of the cable joints. The larger the contact coefficient k is, the higher the temperature of the joint is, the greater the thermal stress, and vice versa. In the load current I = 638A and the ambient temperature Tamb = 25 ℃, change the size of the value of contact coefficient k, calculated to obtain the cable core and surface stress cloth curve shown in Figure 7 and Figure 8, respectively. The stress curve results can be seen:

(a) With the increase of the contact coefficient k, the stress of the conductor and the surface of the cable core increases, and the increase of the stress also increases slightly. Taking the cable core conductor as an example, if the contact coefficient k increases from 1 to 4, the stress at z=2700mm and z=5500mm increases from $2.42062\times107N/m^2$ and $5.99063\times107N/m^2$ to $2.48211\times107N/m^2$ and $6.21261\times107N/m^2$, respectively, which increases by $6.249\times105N/m^2$ and $2.2342\times106N/m^2$, respectively. When the contact coefficient k increases from 10 to 13, it increases by $7.231\times105N/m^2$, respectively.

(b) With the cable core conductor stress distribution is different, the cable surface for the free boundary, the stress distribution is mainly affected by the temperature, the external is not affected by other phase contact medium material, therefore, the cable surface stress curve distribution law and temperature curve distribution law is the same, and z = 4800mm at the cable body surface stress by the contact coefficient k is very small.

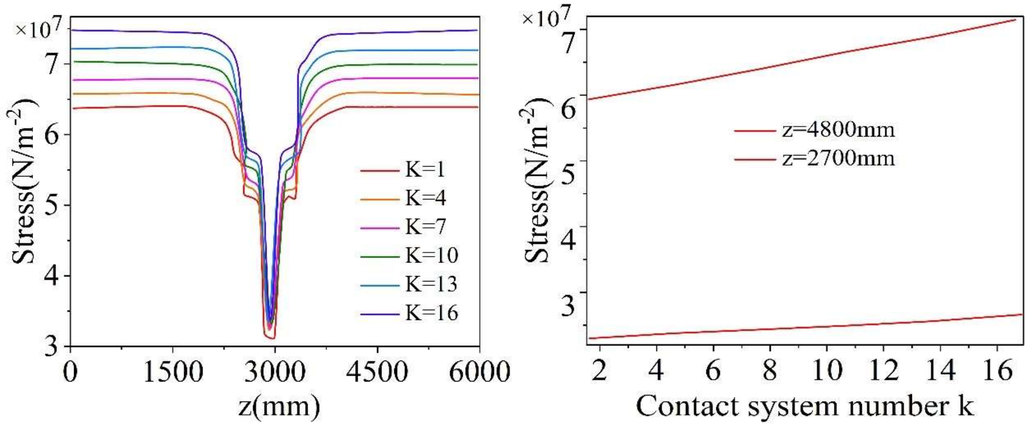

(a) Distribution along the axis (b) z=4800 and 2700mm

Fig. 7. Cable core stress distribution curve

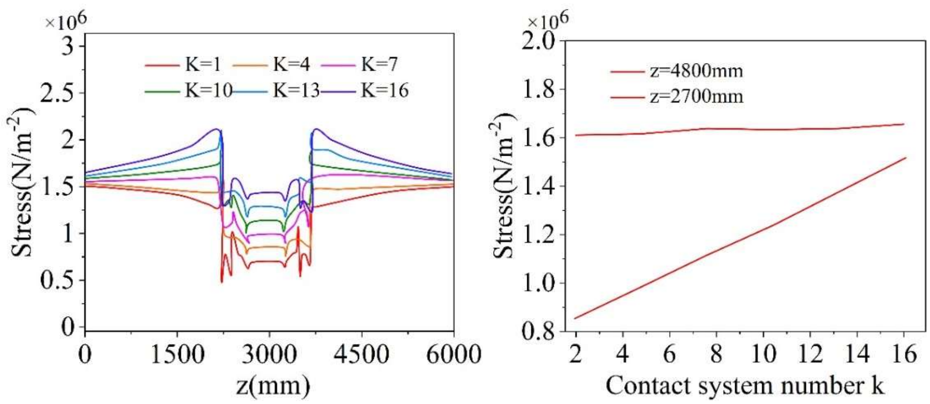

(a) Distribution along the axis (b) z=4800 and 2700mm

Fig. 8. Cable surface stress distribution curve

2) The effect of ambient temperature Tamb on stress characteristics. The higher the ambient temperature, the higher the temperature of the cable, the stress of the cable increases, and vice versa. Keeping the load current I = 638A and contact coefficient k = 7 unchanged, the calculated ambient temperature Tamb were 10, 15, 20, 25, 30 and 35 ℃ cable core and surface stress distribution curve shown in Figure 9 and Figure 10, respectively. The results are shown as follows:

(a) Cable core conductor and surface stress with the ambient temperature Tamb increase and increase, the increase in the amount of ambient temperature Tamb increase between the ratio remains constant. Take the cable core conductor as an example, every 1℃ increase in ambient temperature, z=2700mm and z=4800mm at the cable core conductor stress increased by 87286N/m^2 and 223190N/m^2 respectively.

(b) The difference between the core and surface stresses at z=2700 mm and z=4800 mm are less affected by the change in ambient temperature and are approximately constant.

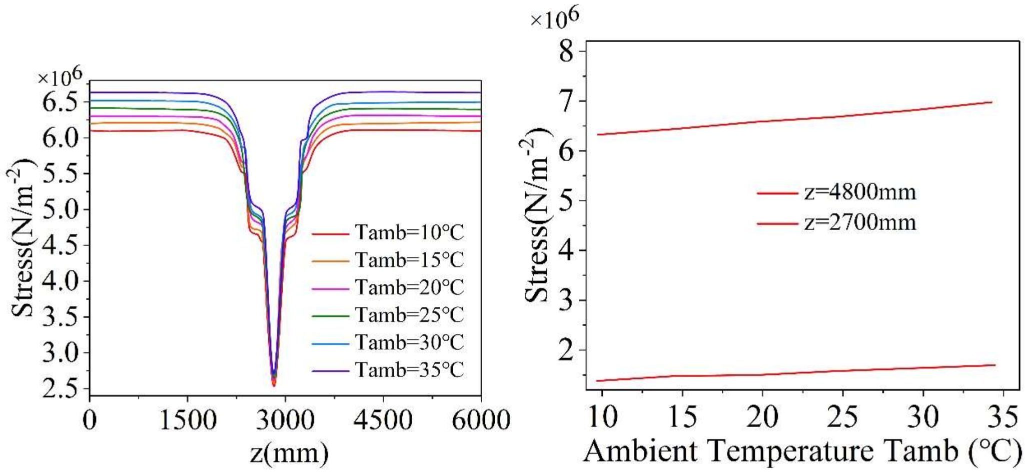

(a) Distribution along the axis (b) z=4800 and 2700mm

Fig. 9. Cable core stress distribution curve

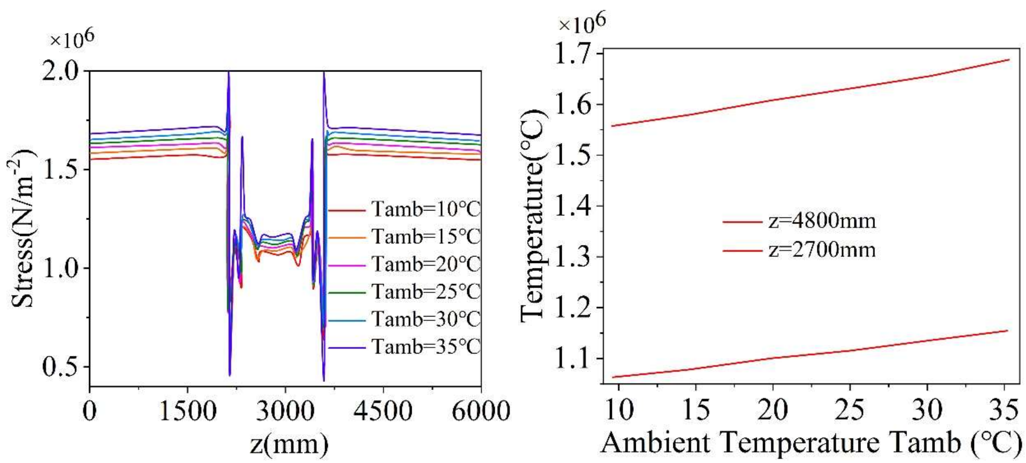

(a) Distribution along the axis (b) z=4800 and 2700mm

Fig. 10. Cable surface stress distribution curve

3.2. Cable thermal characterization

3.2.1. Environment configuration and training.The operating system used for the experimental training is Ubuntul 8.04 system with 32GB of RAM and GPU .NVIDIA GeForce RTX4090.The programming language is Python.4.0.The software libraries used include OpenCV, Pytorch, Pillow and so on.

3.2.2. Comparative analysis of training curve results.The cable temperature and stress distribution values are solved using sequential coupled lines, which form the training dataset, which is put into the RNN network, CNN network, and the proposed Lap-ML-ELM algorithm to complete the training, respectively, and the average Loss value of each training cycle is recorded in order to more intuitively demonstrate the decreasing trend of the Loss value along with the training process, and the Loss curves of the three networks are shown in Fig. 11. Different colors are used to distinguish the loss curves of different network models: the red line represents the RNN network, the orange line represents the original CNN network, and the magenta line represents the Lap-ML-ELM algorithm proposed in this paper. By observing the graphs, it can be clearly found that the absolute value of the loss function of the Lap-ML-ELM algorithm is lower compared to that of the RNN network and the CNN network, no matter in the early stage of training or in the late stage of convergence. In particular, after the number of iterations exceeds 60, the decline rate of the loss curve of the Lap-ML-ELM algorithm slows down, and the reduction of the loss function value decreases, but the overall trend still tends to be 0. Meanwhile, the CNN network starts to slow down the decline rate of the loss function when the iteration reaches about 70 times. The RNN network, on the other hand, reaches its lowest loss value after about 100 iterations.

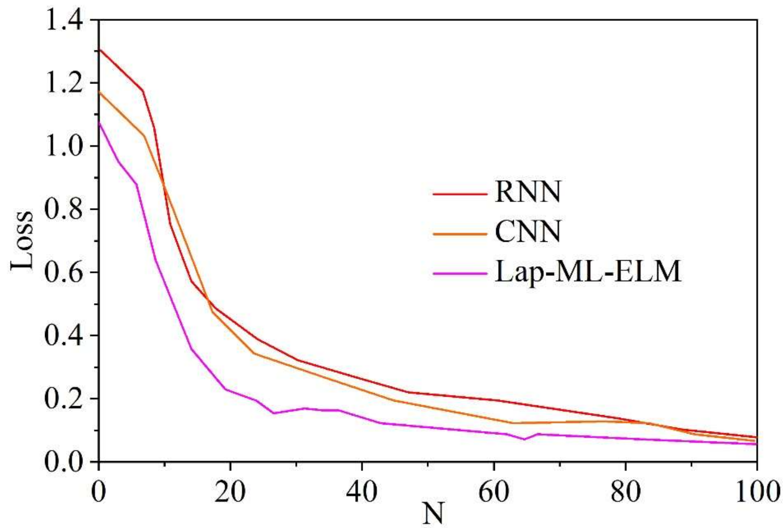

Fig. 11. loss curves of three kinds of networks

Next, the thermal property detection accuracies of the three networks are analyzed, and Fig. 12 shows the thermal property detection Accuracy curves of the three networks. In Fig. 12, the red curve represents the evolution of thermal property detectionaccuracy for CNN networks, the orange curve corresponds to RNN networks, and the magenta curve represents the Lap-ML-ELM algorithm proposed in this paper. It is found that the thermal property detection accuracies curves of the Lap-ML-ELM algorithm are consistently higher than those of the RNN network and the CNN network throughout the training iteration cycle. Especially at the 60th iteration, the thermal property detection accuracies based on the Lap-ML-ELM algorithm have reached a steady state with high accuracy. In contrast, the RNN network reaches stability only at the 30th iteration when the accuracy approaches 0.80. The CNN network, on the other hand, stabilized at the 40th iteration. Summarizing the above analysis, by comparing the changes of the loss curve and the accuracy curve during the training process, it can be concluded that the Lap-ML-ELM algorithm proposed in this paper not only performs well in convergence speed, but also outperforms the other two traditional network models in the detection of the thermal characteristics of the cables, which indicates that on the basis of sequential coupling to solve for the temperature and stress characteristics of the cables, the use of Laplacian This indicates that the thermal property detection performance of the Laplace MLM fusion algorithm is better than the other two traditional network models on the basis of sequential coupling to solve the cable temperature and stress characteristics, which is of great significance for the intelligent management and monitoring of cables.

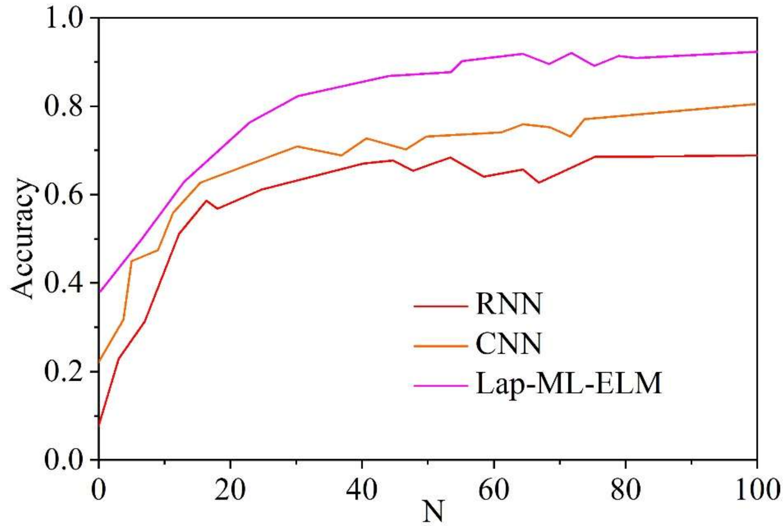

Fig. 12. The thermal characteristics of the three networks detect the accuracy curve

4. Conclusion

Based on the Lap-ML-ELM algorithm, the internal structure of the cable, the article interprets the theory of electric power characteristics in terms of temperature and stress. The structural mechanical properties of different design parameters under thermal and compressive loading conditions are explored to provide data support for cable thermal characterization. The cable temperature and stress distribution values are solved based on sequential coupling, which are put into the model as inputs for training, and the trained model is applied to the real scenario to analyze and process the real-time collected cable data. When the contact coefficient increases, the corresponding temperature and stress of the cable also increase. Under the effect of ambient temperature Tamb, the cable core and surface temperatures also show a single picking increasing trend, while the core and surface stresses are the same. In the whole thermal characteristic detection process, Lap-ML-ELM algorithm performs better than RNN network and CNN network, which indicates that Laplace multilayer Extreme Learning Machine fusion algorithm is able to realize intelligent management and monitoring of cables for the development of electric power enterprises.

Funding

This work was supported by Technology project of funded by State Grid Hebei Electric Power Co., Ltd. (Grant number: KJ2022-016).

References

[1] Medková, D. (2018). The Laplace equation. Boundary value problems on bounded and unbounded Lipschitz domains. Springer, Cham.

[2] Lindqvist, P. (2019). Notes on the stationary p-Laplace equation. Berlin: Springer International Publishing.

[3] Catino, G., Monticelli, D. D., & Roncoroni, A. (2023). On the critical p-Laplace equation. Advances in Mathematics, 433, 109331.

[4] Pan, C., Feng, S., Tao, S., Zhang, H., Zheng, Y., & Ye, H. (2024). Physics-informed neural network for solving Young–Laplace equation and identifying parameters. Physics of Fluids, 36(2).

[5] Mihaylovna, B. A. (2024). SOLUTION OF THE DIRICHLET PROBLEM ON A SPHERE FOR THE LAPLACE EQUATION. Eurasian Journal of Academic Research, 4(6-1), 254-261.

[6] Majić, M. R., Auguié, B., & Le Ru, E. C. (2017). Spheroidal harmonic expansions for the solution of Laplace's equation for a point source near a sphere. Physical Review E, 95(3), 033307.

[7] BatuBara, A. U. (2023). The Application Of The Laplace Transform In The Heat Equation. International Journal of Health Engineering and Technology (IJHET), 1(6).

[8] Shrestha, A., & Mahmood, A. (2019). Review of deep learning algorithms and architectures. IEEE access, 7, 53040-53065.

[9] Pouyanfar, S., Sadiq, S., Yan, Y., Tian, H., Tao, Y., Reyes, M. P., ... & Iyengar, S. S. (2018). A survey on deep learning: Algorithms, techniques, and applications. ACM computing surveys (CSUR), 51(5), 1-36.

[10] Mathew, A., Amudha, P., & Sivakumari, S. (2021). Deep learning techniques: an overview. Advanced Machine Learning Technologies and Applications: Proceedings of AMLTA 2020, 599-608.

[11] Mu, R., & Zeng, X. (2019). A review of deep learning research. KSII Transactions on Internet and Information Systems (TIIS), 13(4), 1738-1764.

[12] Bull, D., Baca, M., & Schenkman, B. (2018). Electrical cable utilization for wave energy converters. Journal of Ocean Engineering and Marine Energy, 4, 171-186

[13] Xu, J., Sun, H., & Cai, S. (2019). Effect of symmetrical broken wires damage on mechanical characteristics of stay cable. Journal of Sound and Vibration, 461, 114920.

[14] Müller, A. C., Blenk, T., Weindl, C., Gerlach, A. K., & Geiger, D. (2020, July). Accelerated Aging of MV Cables as a Function of Grid Utilization. In 2020 IEEE 3rd International Conference on Dielectrics (ICD) (pp. 1-4). IEEE.

[15] Cho, C. E., Lee, O. Y., Kim, S. B., & Kim, K. S. (2021). MV Cable Failure Statistics Analysis and Failure Rate Utilization Method of Prioritization of Diagnosis Targets. KEPCO Journal on Electric Power and Energy, 7(2), 263-268.

[16] Marabaeva, L. V., Kuznetsova, E. G., Hairov, R. R., & Shilkina, T. E. (2022). Features of strategic management of cable industry sustainable development. In Cooperation and Sustainable Development (pp. 1171-1178). Springer International Publishing.

[17] Lu, M. T., Tsai, J. F., Shen, S. P., Lin, M. H., & Hu, Y. C. (2020). Estimating sustainable development performance in the electrical wire and cable industry: Applying the integrated fuzzy MADM approach. Journal of Cleaner Production, 277, 122440.

[18] Qin, X., Wu, G., Lei, J., Fan, F., & Ye, X. (2018). Detecting inspection objects of power line from cable inspection robot LiDAR data. Sensors, 18(4), 1284.

[19] Chen, X., Liu, N., You, B., & Xiao, B. (2016). A novel method for surface defect inspection of optic cable with short-wave infrared illuminance. Infrared Physics & Technology, 77, 456-463.

[20] Yang, L., Fan, J., Liu, Y., Li, E., Peng, J., & Liang, Z. (2020). A review on state-of-the-art power line inspection techniques. IEEE Transactions on Instrumentation and Measurement, 69(12), 9350-9365.

[21] Zhao, L., Li, Y., Xu, Z., Yang, Z., & Lü, A. (2014). On-line monitoring system of 110 kV submarine cable based on BOTDR. Sensors and Actuators A: Physical, 216, 28-35.

[22] Song, Y., Chen, W., Wan, F., Zhang, Z., Du, L., Wang, P., ... & Huang, H. (2022). Online multi-parameter sensing and condition assessment technology for power cables: A review. Electric Power Systems Research, 210, 108140.

[23] Hu, Y., & Liu, K. (2017). Inspection and monitoring technologies of transmission lines with remote sensing. Academic Press.

[24] Govindarajan, S., Morales, A., Ardila-Rey, J. A., & Purushothaman, N. (2023). A review on partial discharge

diagnosis in cables: Theory, techniques, and trends. Measurement, 216, 112882.

[25] Gotts, C., Hall, B., Beaumont, O., Chen, Z., Cleaver, W., England, J., ... & Thornton, B. (2022). Development of a prototype autonomous inspection robot for offshore riser cables. Ocean Engineering, 257, 111485.

[26] Li, X., Gao, C., Guo, Y., He, F., & Shao, Y. (2019). Cable surface damage detection in cable-stayed bridges using optical techniques and image mosaicking. Optics & Laser Technology, 110, 36-43.

[27] Kong, X., Liu, Z., Liu, H., Hu, J., & Deng, L. (2024). Recent advances on inspection, monitoring, and assessment of bridge cables. Automation in Construction, 168, 105767.

[28] Yücel, M. K., Legg, M., Kappatos, V., & Gan, T. H. (2017). An ultrasonic guided wave approach for the inspection of overhead transmission line cables. Applied Acoustics, 122, 23-34.

[29] Zhang, D., Li, S., Cao, B., & Kang, Y. (2022, September). Review of defect inspection method of cable terminals. In 2022 3rd International Conference on Advanced Electrical and Energy Systems (AEES) (pp. 270-274). IEEE.

[30] Yang, W., Huang, J., Wang, P., Chen, X., Zhou, Y., Su, Q., ... & Xia, C. (2021). An intelligent distributed sensor developed for power cable external damage monitoring. Procedia Computer Science, 183, 166-174.

[31] Tang, W., Brown, K., Flynn, D., & Pellae, H. (2018, October). Integrity analysis inspection and lifecycle prediction of subsea power cables. In 2018 Prognostics and System Health Management Conference (PHM-Chongqing) (pp. 105-114). IEEE.

[32] Uddin, M. N., Rashid, M. M., Mostafa, M. G., Nithe, N. A., Aziz, M. A., & Halder, S. (2016). Design & Development of Electric Cable Inspection. Global Journal of Research In Engineering.

[33] Kim, J., Seo, D. W., Jung, K. S., & Park, K. T. (2020). Evaluating Performance of Cable-Inspection Robot in Cable-Supported Bridge. Journal of the Korea institute for structural maintenance and inspection, 24(1), 74-79.

[34] Jia, Z., Tian, Y., Liu, Z., & Fan, S. (2022). Condition assessment of the cable trench based on an intelligent inspection robot. Frontiers in Energy Research, 10, 860461.

[35] You, Y., Zheng, Y., Huang, K., He, Y., Huang, Z., & Zhan, L. (2024, September). Development of a Small-Sized Urban Cable Conduit Inspection Robot. In Actuators (Vol. 13, No. 9, p. 349). MDPI.

[36] M. Budylin,S. B. Levin & T. S. Yurova. (2024). Asymptotics of the Solution of the Dirichlet Problemfor the Laplace Equation in a Strip with Thin Branches. Mathematical Notes(3),432-445.

[37] S. O. Gladkov. (2024). On Some Class of Solutions to the Two-Dimensional Laplace Equation on a Three-Dimensional Manifold. Siberian Mathematical Journal(6),1423-1428.

[38] Guillaume Valette. (2024). On the Laplace equation on bounded subanalytic manifolds. Calculus of Variations and Partial Differential Equations(9),236-236.